Geosci. Model Dev. Discuss., 5, 4355–4393, 2012
www.geosci-model-dev-discuss.net/5/4355/2012/
doi:10.5194/gmdd-5-4355-2012

Geoscientific Model Development Discussions

Modeling short wave solar radiation using the JGrass-NewAge System

G. Formetta[1], R. Rigon[1], J. L. Chávez[2], and O. David[2,3]

[1]University of Trento, 77 Mesiano St., 38123 Trento, Italy
[2]Dept. of Civil and Environmental Engineering, Colorado State University, Fort Collins, CO, USA
[3]Agricultural Systems Research Unit, USDA-ARS-NPA-ASRU 2150 Centre Ave., Fort Collins, CO 80526, USA

Received: 23 October 2012 – Accepted: 30 November 2012 – Published: 18 December 2012

Correspondence to: G. Formetta (formetta@ing.unitn.it)

Published by Copernicus Publications on behalf of the European Geosciences Union.

Abstract

This paper presents two new modelling components based on the Object Modelling System v3 for the calculation of the shortwave incident radiation ($\hat{R}_{sw}\downarrow$) on complex topography settings, and the implementation of several ancillary tools. The first component, NewAGE-SwRB, accounts for slope, aspect, shadow and the topographical information of the sites, and use suitable parametrisation for obtaining the cloudless irradiance. A second component, NewAGE-DEC-MOD's is implemented to estimate the irradiance reduction due to the presence of clouds, according to three parameterisations. To obtain a working modelling composition, suitable to be compared with ground data at measurement stations, the two components are connected to a Kriging component, and, with the use of a further component NewAGE-V (verification package), the performance of modeled ($\hat{R}_{sw}\downarrow$) is quantitatively evaluated. The two components (and the various parametrisations they contain) are tested using the data from three basins catchments, and some simple verification test is made to assess the goodness of the methods used. The components are part of a larger system, JGrass-NewAGE, their input and outputs are given as geometrical objects immediately visualisable in a GIS (for instance the companion uDig), and can be used seamlessly with the various modelling solutions available in JGrass-NewAGE for the estimation of long wave radiation, evapotranspiration, and snow melting, as well as stand-alone components to just estimate shortwave radiation for various uses. The modularity of the approach is shown to be extensible to more accurate physical-statistical studies aimed to assess in deep the components performances and extends spatially their results, without the necessity of recoding any part of the component but just making using of connective scripts.

1 Introduction

Solar radiation at the top of the atmosphere is just function of Sun activity but, in the case of hydrological studies, the solar constant, $I_{sc} \sim 1367$ [W m^{-2}], is used as

GMDD

5, 4355–4393, 2012

a suitable approximation of the irradiance at the top of the atmosphere. This value represents the maximum irradiance when the solar beam hits orthogonally the Earth, and reduction of irradiance due to latitude and longitude, the day of the year, and the hour, is necessary, and can be easily calculated with the desired approximation, e.g. Iqbal (1983) and Liou (2002).

In the absence of clouds, solar radiation arrives at the Earth's ground surface in two classes. Direct radiation ($S\downarrow^*$) is that part of the solar beam which arrives at the surface without any interaction with the Earth's atmosphere. Diffuse radiation ($d^*\downarrow$) is shortwave radiation scattered downwards back to the Earth's surface after hitting molecules of the atmospheric gases and aerosols. In this paper we will call the sum of $S\downarrow^*$ and $d^*\downarrow$, total Shortwave Radiation at the ground ($R^*\downarrow_{sw}$).

When it is assumed that shortwave radiation hits rugged terrains, geometrical corrections can be applied to obtain the theoretical irradiances that hit the tilted terrain surface in absence of the atmosphere before accounting for the attenuations due to scattering. These quantities are therefore very far from the real radiation measured by instruments on the ground for the effects introduced by atmosphere's scattering, reflections, absorptions (Liou, 2002) and landscape multiple reflections, and will be denoted $S\downarrow$, $d\downarrow$ and $R_{sw}\downarrow$ through the paper, which shows an implementation of Corripio (2003) algorithms.

With the development of modern computing power efficient methods were developed to estimate irradiance over vast mountain regions. Those studies were based on the elaboration of digital elevation models (DEMs) from which terrain's characteristics were automatically derived, and used algorithms of various degree of complexity. A long series of studies parametrize $R_{sw}\downarrow$ since the 1960'ies which are well reviewed in Duguay (1993). Among many, Dozier and Frew (1990) were the first to used DEMs for rapid estimation of $S\downarrow^*$ and $d^*\downarrow$ solar radiation; Dubayah (1994) presented a method that combines a simplified $d\downarrow$ radiation model with the topographic shading and the sky view field, and discusses various levels of complexities that can be introduced in the estimation of radiation beams. Ranzi and Rosso (1995) used Stokes' theorem

GMDD
5, 4355–4393, 2012

to estimate $S\downarrow$ for a whole basin area; Gubler et al. (2012) tried to assess the inherent error in the estimation of the short wave incoming solar radiation. The above approaches, were aimed to computational efficiency and simplified parameterisations, and produced several software packages that offer different methodologies, such as SolarFlus (in ArcInfo GIS) (Dubayah and Paul, 1995; Hetrick et al., 1993), Solar Analyst (Fu and Rich, 2000), SRAD (by Moore, 1992, and documented in Wilson and Gallant, 2000), Solei (Miklánek, 1993) or r.sun (Hofierka and Suri, 2002), and often integrate the models in GIS. Our modelling, making treasure of these previous efforts, is also in line with those that tried to respond to the increase demand of modularity and interchangeability in hydrological and biophysical models that have been developed in the last decades. This trend is widespread in industrial software and gained momentum also in scientific research in environmental fields (e.g. Jones et al., 2001; David et al., 2002; Donatelli et al., 2006; Rizzoli et al., 2005).

Finally, our effort, in particular uses the Object Modelling System v.3.0 (David et al., 2002, 2010) components's framework and seamlessly integrates ion the Spatial Toolbox of the uDig GIS, which is based upon OMS3.

This paper introduces and tests model components for the estimation of the direct solar radiation which are part of a larger modeling effort called JGrass-NewAGE (Formetta et al., 2011, 2013) with the goal of estimating all the components of the hydrological cycle for medium to large catchments. Of this goal, short wave radiation is an important part since it is necessary for the estimation of long wave radiation, evapotranspiration and snow cover evolution. However, the modelling components developed work also stand-alone, for any possible use.

2 The JGrass-NewAGE component for the estimation of the shortwave radiation budget (NewAGE-SwRB)

This component, NewAGE-SwRB (or simply SwRB in the following) was built to be able to simulate the direct shortwave radiation budget in multiple points in a landscape,

GMDD
5, 4355–4393, 2012

and to provide inputs to hydrological components independently of their geographical structure (either implementing fully distributed, semi-distributed or lumped concepts). Hence, from a spatial point of view, the output of SwRB can be a raster (the results are provided for each pixel of the computational domain) or vectorial (the results are provided only in some points of the computational domain) according to the the modeller's needs, and in Open GIS Consortium standard formats (as GridCoverage and shapefiles, respectively). For the various use, the component was re-used to be able to provide results using a generic hourly, sub-hourly and daily time step, according to the users' specifications.

While not trivial to obtain, the geometrical elaboration of the radiation that returns the incoming solar radiation on a tilted plane, is given for granted, and estimated according to the elegant solution provided by Corripio's algorithms (Corripio, 2002, 2003). Therefore in the following is assumed that the solar constant, I_{sc} has been spatially corrected to account for the geometry and the position of the landscape underneath, to give a "corrected" solar constant, $\hat{I}_{sc}$.

2.1 Direct Solar Radiation under cloudless sky conditions

Therefore, the incident $R\downarrow_{sw}$, on an arbitrary sloping surface in a point, under cloudless sky condition is given by Corripio (2002):

$$R\downarrow_{sw} = C_1 \cdot \hat{I}_{sc} \cdot E_0 \cdot \cos(\theta_s) \cdot (T_s + \beta_s) \cdot \psi \quad (1)$$

in which:

– C_1 = 0.9751 is the fraction of solar radiation that is included between 0.3 µm and 3.0 µm wavelength

GMDD
5, 4355–4393, 2012

– E_0 [–] is a correction factor related to the Earth's orbit eccentricity computed according to Spencer (1971):

$$E_0 = 1.00011 + 0.034221\cos(\kappa) + 0.00128\sin(\kappa) + 0.000719\cos(2\kappa) + 0.000077\sin(2\kappa) \quad (2)$$

$$\kappa := 2\pi \cdot \left(\frac{N-1}{365}\right) \quad (3)$$

where κ is the day angle [rad] and N is the day number of the year (N = 1 on 1 January, N = 365 on 31 December);

– T_s [–], product of the atmospheric transmittances, is defined as:

$$T_s := \tau_r \cdot \tau_0 \cdot \tau_g \cdot \tau_w \cdot \tau_a \quad (4)$$

where the τ functions are the transmittance functions for Rayleigh scattering, ozone, uniformly mixed gases, water vapour and aerosols, respectively. They are computed for each point as defined in the last part of this section.

– β_s [m] is a correction factor for increased transmittance with elevation z [m] defined according to Corripio (2002):

$$\beta_s = \begin{cases} 2.2 \times 10^{-5} \cdot z_p & \text{if } z \le 3000 \text{ m} \\ 2.2 \times 10^{-5} \cdot 3000.0 & \text{if } z > 3000 \text{ m} \end{cases} \quad (5)$$

– θ_s [rad] is the angle between the Sun vector and the surface plane (Corripio, 2003); for a horizontal surface $\theta_s = \theta_z$ where θ_z is the zenith angle;

– ψ_s is the shadows index that accounts for the sun or shadow of the point under analysis, and is modelled according to Corripio (2003):

$$\psi_s = \begin{cases} 1 & \text{if the point p is in the sun} \\ 0 & \text{if the point p is in the shadow} \end{cases} \quad (6)$$

GMDD
5, 4355–4393, 2012

The atmospheric transmittances in Eq. (4) are estimated according to Bird and Hulstrom (1981) and Iqbal (1983) to result functions of the atmospheric pressure, the ozone layer thickness, the precipitable water amount, the zenith angle and visibility, which are eventually taken in this paper as fixed values, according to the literature values reported in Table 1.

The transmittance function for Rayleigh scattering τ_r [–] is estimated as:

$$\tau_r = \exp\left[-0.0903 \cdot m_a^{0.84} \cdot (1 + m_a - m_a^{1.01})\right] \quad (7)$$

where m_a [–] is the relative air mass at actual pressure defined as:

$$m_a := m_r \cdot \left(\frac{p}{1013.25}\right) \quad (8)$$

in which p [mbar] is the local atmospheric pressure, m_r [–] relative optical air mass:

$$m_r = \frac{1.0}{\cos(\theta_s) + 0.15(93.885 - (180/2\pi)\theta_s)^{-1.253}} \quad (9)$$

The transmittance by ozone τ_o [–] is defined as:

$$\tau_o = 1.0 - \left[0.1611 l_{oz} m_r (1.0 + 139.48 l_{oz} m_r)^{-0.3035} - \frac{0.002715 l_{oz} m_r}{1.0 + 0.044 l_{oz} m_r + 0.0003 (l_{oz} m_r)^2}\right] \quad (10)$$

where l_{oz} [cm] is the vertical ozone layer thickness, and the coefficients have the appropriate dimensionality ti make τ_0 dimensionless.

Transmittance by uniformly mixed gases τ_g [–] is modelled as:

$$\tau_g = \exp\left[-0.0127 \cdot m_a^{0.26}\right] \quad (11)$$

GMDD
5, 4355–4393, 2012

Transmittance by water vapour τ_w is estimated as:

$$\tau_w = 1.0 - \frac{2.4959\, w\, m_r}{(1.0 + 79.034\, w\, m_r)^{0.6828} + 6.385\, w\, m_r} \quad (12)$$

where w [cm] is precipitable water in cm calculated according to Prata (1996).

Finally, the transmittance by aerosols τ_a [–] is evaluated as:

$$\tau_a = \left[0.97 - 1.265 \cdot V^{-0.66}\right]^{m_a^{0.9}} \quad (13)$$

where V [km] is the visibility, i.e. an estimation of the visibility extent as in Corripio (2002).

2.2 Diffuse solar radiation under cloudless sky conditions

The modelling of the diffuse component of solar radiation, $d\downarrow$ follows Iqbal (1983):

$$d\downarrow = (d\downarrow_r + d\downarrow_a + d\downarrow_m) \cdot V_s \quad (14)$$

where $d\downarrow_r$, $d\downarrow_a$ and $d\downarrow_m$ are the diffuse irradiance components after the first pass through the atmosphere due to the Rayleigh-scattering, the aerosol-scattering and multiple-reflection, respectively.

The Rayleigh-scattered diffuse irradiance is computed as:

$$d\downarrow_r = \frac{0.79 \cdot \cos(\theta_z) \cdot I_{sc} \cdot E_0 \cdot \tau_o \cdot \tau_g \cdot \tau_w \cdot \tau_{aa} \cdot (1 - \tau_r)}{2.0 \cdot (1.0 - m_a + m_a^{1.02})} \quad (15)$$

where τ_{aa} is the transmittance of direct radiation due to aerosol absorptance modelled as:

$$\tau_{aa} = 1.0 - (1 - \omega_0) \cdot (1 - m_a + m_a^{1.06}) \cdot (1.0 - \tau_a) \quad (16)$$

GMDD
5, 4355–4393, 2012

where $\omega_0 = 0.9$ [–] is the single-scattering albedo fraction of incident energy scattered to total attenuation by aerosols (Hoyt, 1978).

The aerosol-scattered diffuse irradiance component is defined as:

$$d\downarrow_a = \frac{0.79 \cdot I_{sc} \cdot \cos(\theta_z) \cdot E_0 \cdot \tau_o \cdot \tau_g \cdot \tau_w \cdot \tau_{aa} \cdot F_c \cdot (1 - \tau_{as})}{1 - m_a + m_a^{1.02}} \quad (17)$$

where $\tau_{as} := \tau_a \tau_{aa}^{-1}$ and F_c is the fraction of forward scattering to total scattering (Iqbal, 1983, $F_s = 0.84$ if no information about the aerosols are available,).

The diffuse irradiance from multiple reflections between the earth and the atmosphere is computed as:

$$d\downarrow_m = \frac{(R\downarrow sw + d\downarrow_r + d\downarrow_a) \cdot \alpha_g \cdot \alpha_a}{1.0 - \alpha_g \cdot \alpha_a} \quad (18)$$

where α_g is the albedo of the ground and α_a is the albedo of the cloudless sky computed as:

$$\alpha_a = 0.0685 + (1.0 - F_c) \cdot (1 - \tau_{as}) \quad (19)$$

Finally V_s is the sky view factor, i.e. the fraction of sky visible in a point, computed using the algorithm presented in Corripio (2002).

2.3 The shortwave radiation correction for cloudy sky, DEC-MOD's

The radiation components presented in the previous subsections are computed under the hypothesis of cloudless sky conditions. To account for the presence of clouds, some models found in the literature were denominated decomposition models. The procedure described here is in line with Helbig et al. (2010). It corrects the clear sky direct and diffuse irradiance by means of adjustment coefficients and the clear sky irradiances so that, for any point:

$$S\downarrow^* := c_s \cdot S\downarrow \quad (20)$$

GMDD
5, 4355–4393, 2012

is the corrected irradiance for direct shortwave radiation (and c_s is the correction coefficient for $S\downarrow$), and

$$d\downarrow^* := c_d \cdot d\downarrow \tag{21}$$

is the corrected irradiance for the diffuse shortwave radiation (and c_d is the correction coefficient for $d\downarrow$). The coefficients of reduction are made dependent upon the global shortwave irradiance measured at the available stations as suggested by Orgill and Hollands (1977), Erbs et al. (1982) and Reindl et al. (1990), so that, for any station, i:

$$\hat{R}_{sw}\downarrow_i = S\downarrow_i^* + d^*\downarrow_i \tag{22}$$

$$d^*\downarrow_i = (k_d)_i \hat{R}_{sw}\downarrow_i \tag{23}$$

equation which also define k_d, the ratio between the diffuse shortwave irradiance and the shortwave total irradiance. Therefore, at stations:

$$(c_d)_i = \frac{\hat{R}_{sw}\downarrow_i \cdot k_d}{d\downarrow_i} \tag{24}$$

and

$$(c_s)_i = \frac{\hat{R}_{sw}\downarrow_i \cdot (1 - (k_d)_i)}{S\downarrow_i} \tag{25}$$

Clearly k_d becomes the key parameter to be determined to close, for the stations, the estimation of the cloudy irradiances. To this goal, we use here three different parameterisations.

– Erbs et al. (1982) estimated k_d for latitudes between 31 and 42 degrees North, using hourly data from five irradiances measurement stations in the USA:

$$k_d = \begin{cases} 1.0 - 0.09\,k_t & \text{if } k_t \le 0.22 \\ 0.951 - 0.1604 k_t + 4.388\,k_t^2 - 16.638\,k_t^3 + 12.336\,k_t^4 & \text{if } 0.22 < k_t \le 0.80 \\ 0.165 & \text{if } k_t > 0.80 \end{cases}$$

GMDD
5, 4355–4393, 2012

(26)

– Reindl et al. (1990) estimated the diffuse fraction k_d known k_t using data measured in USA and Europe (latitude between 28–60 degrees N) and provided this relations:

$$k_d = \begin{cases} 1.02 - 0.248 \cdot k_t & \text{if } k_t \leq 0.30 \\ 1.45 - 1.67 k_t & \text{if } 0.30 < k_t \leq 0.78 \\ 0.147 & \text{if } k_t > 0.78 \end{cases} \quad (27)$$

– Boland et al. (2001) using data from Victoria, Australia, provided the exponential relation:

$$k_d = \frac{1.0}{1.0 + e^{7.997(k_t - 0.586)}} \quad (28)$$

In turn Eq. (22) above is completely determined by the knowledge of the clearness sky index, k_t [–], which is defined as:

$$k_t := \frac{\hat{R}_{sw}\downarrow}{\hat{I}_{sc} \cdot E_0 \cdot \cos(\theta_s)} \quad (29)$$

Using the above equations a set of adjustment coefficients, c_s and c_d for beam and diffuse radiation component are obtained for the measurements station. To be extended to any spatial point, they need to be extrapolated to all the points of interest (where incoming shortwave solar radiation is not measured). This is accomplished in NewAGE-DEC-MOD's by using the JGrass-NewAge Kriging component (Formetta et al., 2011) and using a simple kriging algorithm (Goovaerts, 1997).

GMDD
5, 4355–4393, 2012

3 Applications

The capability of the model was tested by joining with the appropriate OMS script (available in the complementary material) four JGrass-NewAGE components: the SwRB, the (Radiation Decomposition model) DEC-MOD's, the Kriging and the NewAGE-V (Verification) package connected as illustrated in Fig. 1.

Below we described the basins used for the verification, comments their data, and illustrate the procedure of verification.

3.1 Reference catchments

Three different river basins were used: Little Washita river basin (Oklahoma, US), Fort Cobb river basin (Oklahoma, US) and Piave radiation dataset (Veneto, Italy). As presented in the next subsections, differences between the two places in elevation range, number of monitoring points, latitudes, and complexity of the topography are substantial.

The Little Washita river basin (611 km^2) is located in southwestern Oklahoma, between Chickasha and Lawton and its main hydrological and geological features are presented in Allen and Naney (1991). The elevation range is between 300 and 500 m above sea level, the main land use are range, pasture, forest, cropland. The mean annual precipitation is 760 mm and the mean air temperature is 16 degrees Celsius. Seventeen meteorological stations of the ARS Micronet (http://ars.mesonet.org/) are used for the simulations and for each stations are available five minutes measurements of: air temperature at a height of 1.5 m, relative humidity at a heigth of 1.5 m and incoming global solar radiation. The data for the year 2002 were summed to an hourly time step to be used in the simulations. The meteorological stations main features are reported in Table 2 and Fig. 5 shows their location.

The Fort Cobb river basin (813 km^2) is located in southwestern Oklahoma and an exhaustive description is given in Rogers (2007). The elevation range is between 400 and 570 m above the sea level, the main land usage are cropland, range, pasture, forest,

GMDD
5, 4355–4393, 2012

water. The long record mean annual precipitation is 816 mm and the mean annual air temperature is 18 degrees Celsius. Eight meteorological stations of the ARS Micronet (http://ars.mesonet.org/) are used for the simulations. The data for the year 2006 were accumulated to an hourly time step and used in the simulations.

The meteo stations main features are reported in Table 3 and the top of Fig. 6 shows their position.

The Piave river basin area (3460 km^2) is located in the north-eastern part of the Italian peninsula. The elevation range is between 700 and 3160 m above sea level, the main soil uses are: (i) crops up to 500 m a.s.l., (ii) evergreen and deciduous forests at elevation between 500 and 1800 m a.s.l. and (iii) alpine pasture and rocks at higher elevations. The mean annual precipitation is around 1500 mm and the mean air temperature is 10 ˚C.

Seventeen meteorological stations are used for the simulations and for each stations are available five minutes measurements of: air temperature at a heigth of 1.5 m, relative humidity at a heigth of 1.5 m and incoming global solar radiation. The data for the year 2010 were summarized to an hourly time step and were used in the simulations. The meteo stations main features are reported in Table 4 and the top of Fig. 7 shows their position.

3.2 Data analysis

As presented in Tovar et al. (1995), the solar radiation measurement over a flat and homogeneous landscape are well correlated and the correlation decrease with the distances from the considered station. If we move the analysis on the complex topography landscape the correlation between solar radiation measurement decrease respect to the flat landscape. This is confirmed in the analyses datasets. In particular, we focus our attention on the Little Washita river basin, which can be considered a flat and homogenous landscape river basin, and on Piave river basin which can be considered complex topography landscape river basin. The correlogram for two station on Little Washita river basin and two station on Piave river basin are presented in Fig. 2 at the

GMDD
5, 4355–4393, 2012

top and at the bottom, respectively. For Little Washita river basin the correlogram between measurement stations shows high values through the whole basin. The Piave river basin is much more rugged and its correlogram, in agreement with other literature findings (e.g. Tovar et al., 1995; Long and Ackerman, 1995), is much lower. Moreover the correlogram on Piave river basin decreases faster than the correlogram on Little Washita river basin, and this certainly would imply a minor predictive capability of quantities based on measurements statistics.

3.3 Plan of simulations and verification method

The SwRB component just estimate for any point of a basin the incoming radiation. It does not require any calibration, once the four parameters in Table 1 are assigned according to literature values. These outputs, however, do not correspond to a measured quantity but to an intermediate step of the calculations. Just the data coming out from the DEC-MOD's component correspond to measured quantities, and, actually, this component uses the measured quantity to estimate the attenuation coefficients. Therefore to allow some validation, we divided any of the group of measurements stations into two subgroup: one used for the estimation of the coefficients, (say C-set), and the other for the verification of the results, (say V-set). Stations used for verification are in bold letters in Tables 2, 3 and 4. More complex verification strategies could be used, as described in the discussion section, but their application is beyond the scope of the present work.

Therefore, for any of the three basins is applied:

- the SwRB in the subset of the measurement stations. The result for this step is the computation of the clear sky surface shortwave radiation. Inputs and outputs of the model are reported in Table 1. The main parameters value used in the simulations are reported in Table 1 according to Iqbal (1983) and Corripio (2002);
- the DEC-MOD's presented in the previous section and estimation of the coefficients c_s and c_d. Inputs and outputs of the model are reported in Fig. 1;

GMDD
5, 4355–4393, 2012

– the ordinary Kriging component (Formetta et al., 2011) to extrapolate the coefficients c_s and c_d for the set of stations left for verification (in bold in Tables 2, 3 and 4);

– an estimate of the shortwave incoming solar radiation under generic sky condition in the V-set (SwRB-Allsky, which multiply the SwRB output by the correction coefficients kriging output for the V-Set stations);

– the verification component NewAGE-V (Formetta et al., 2011) to evaluate the performance of the model.

For the simulations of this paper, the Erbs model was used in the case of Piave river basin and Reindl model was used for Little Washita and Fort Cobb catchments.

For verification we used three index of performances:

– mean absolute error (MAE):

$$\mathrm{MAE} = \frac{1}{N} \cdot \sum_{i}^{N} |S_i - O_i| \tag{30}$$

where N is the number of records of the time-series, O are the observed values and S are the simulated values. MAE is expressed in the same units of O and S, and is zero for perfect agreement between observations and estimates.

– Percentual bias (PBIAS):

$$\mathrm{PBIAS} = 100 \cdot \frac{\sum_i^N (S_i - O_i)}{\sum_i^N O_i} \tag{31}$$

PBIAS measures the average tendency of the simulated values to be larger or smaller than their observed ones. The optimal value of PBIAS is zero, with low-magnitude values indicating accurate model simulation.

GMDD
5, 4355–4393, 2012

– Kling Gupta Efficiency (KGE) as reported in Gupta et al. (2009):

$$KGE = 1 - \sqrt{(R-1)^2 + (A-1)^2 + (B-1)^2} \quad (32)$$

in which R represents the linear correlation coefficient between the simulated (S) and measured (O) values, A and B are, respectively expressed in Eqs. (21) and (22):

$$A = \frac{\sigma_o}{\sigma_s} \quad (33)$$

where σ_o is the observed standard deviation value and σ_s is the simulated standard deviation value;

$$B = \frac{\mu_s - \mu_o}{\sigma_o} \quad (34)$$

where μ_s and μ_o are the means of simulated (S) and measured (O) values. For this index, the best agreement is obtained with the value 1.

The Kriging package can utilise the most common variogram models (spheric, linear, exponential, gaussian). However, for these cases below, a linear model was used.

3.4 Results

Results are analysed separately for the three case studies. They confirm the results found in the literature, and reveal a reasonable agreement between measured and simulated data.

3.4.1 Results for Little Washita river basin

Figure 5 shows the scatter plot between the modelled and the measured total incoming solar radiation in the four stations of the V-set.

GMDD
5, 4355–4393, 2012

Table 5 shows the result of the NewAge-V which accepts in input measured and modelled time series and provides as output the user defined goodness of fit indexes.

3.4.2 Results for Fort Cobb river basin

For the Fort Cobb river, the same procedure presented for the Little Washita river basin was followed.

Figure 6 shows the scatter plot between the modelled and the measured total incoming solar radiation in the four V-set stations. Table 6 show the results in term of goodness of fit indices for the V-set.

3.4.3 Results for Piave river basin

For the Arabba river is repeated the same procedure presented for the Little Washita river basin. The decomposition model used in this case is Reindl et al. (1990). Figure 7 shows the scatter plot between the modelled and the measured total incoming solar radiation in the four V-set. Table 7 show the results in term of goodness of fit indexes for the same set of stations.

4 Discussion

4.1 About SwRB and DRM components' predictive capabilities

The model applications are performed in case studies where topography has different characteristics: (a) two cases presented gentle topography and high density measurement network (for the experimental Little Washita and Fort Cobb watersheds) (b) the other case presented a typical case of hydrological basin with complex topography, high elevation range and few monitoring stations.

GMDD
5, 4355–4393, 2012

In all the cases the model was able to simulate the global shortwave solar radiation showing relatively good goodness of fit indices presented in Tables 5 and 6 for Little Washita and Fort Cobb, respectively and in Table 7 for the Arabba river basin.

The model performs with the similar and acceptable accuracy both for Little Washita and Fort Cobb river basin. The result is confirmed by the goodness of fit indices and by the graphical analysis.

The model performance deteriorated in the Arabba case study. This could be due to the effect of the complex topography on the computation of the clear sky solar radiation but also to the lower measurements stations density in high elevation zones.

Because of this topographic condition the increasing measurement data uncertainty about the temperature and humidity influenced the atmospheric transmittance computations. This is confirmed also by the data analysis: for the Piave river basin measurements shows lower correlation respect, for example, the correlation between measurements on the Little Washita river basin, where the gentle topography does not play a crucial rule.

Regardless, the model, also in the case of complex topography watershed was able to reproduce well the shortwave solar radiation. The PBIAS index was equal to 14.80 in the worst case. According the hydrological model classification based on PBIAS index, presented in Van Liew et al. (2005) and Stehr et al. (2008), the results achieved in our study are classified as "good" and therefore the solar radiation model is suitable to be used to estimate incoming shortwave solar radiation.

4.2 About the possibilities open by the components' structure of JGrass-NewAGE

Since the goal of the paper was to show how the components work, the statistical analysis of the results was maintained to a simple level. One more accurate procedure of testing of the components performances would be to apply a "Jack-knife" procedure to estimate errors (as proposed by Quenouille, 1956; Miller, 1974). In this procedure, the V-set, would vary among all the stations and an overall statics could be delineated.

GMDD
5, 4355–4393, 2012

According to Tovar et al. (1995) and Long and Ackerman (1995) studies, the influence of the aspect of the measurements station could have been identified. This operation and analysis, indeed time consuming, can be made, simply by adding a Jack-Knife component to the structure of the model at "linking time", i.e. using the script that connects the components. As presented in Fig. 3, by using the encapsulation properties of OMS, no modification of the core components is needed to accomplish this task.

Other components, in the set of the New-AGE system (e.g. Formetta et al., 2011), allow to perform parameter calibration. In this paper no calibration was performed of the four parameter (in Table 1) needed to run the SwRB component. However, it can be easily envisioned, the use of, for instance, the particle swarm NewAge component (Formetta et al., 2011) for automatic calibration. In this case the diagram of linked components would be the one shown in Fig. 4.

Eventually, the four parameters can become variable in space, and, in this case, would become reasonable to use the Kriging spatial interpolators to give their spatial structure. This would allow for studying the spatial variability of radiative transmittance with position or other characteristics as height, aspect and slope of the terrain.

All of these simulations (Formetta et al., 2013) do not require any rewriting of the code, except the adjustment of the scripts to execute them. At each addition of complexity, derived from adding a component or making spatial a parameter set, the improvement on the final results can be objectively determined with the use of the goodness of fit component, and the user can objectively judge if, with the present parameterisations, the introduction of complexities is worthwhile.

5 Conclusions

The goal of this paper was to present a set of hydrological components to estimate the shortwave incoming solar radiation present in the JGrass-NewAGE system. These components use Object Modelling Sytem v3 to implement encapsulation and other

GMDD
5, 4355–4393, 2012

object oriented features that make possible a flexible modelling structure apt to investigate many scientific questions with a minimum of effort.

The core components presented cover: the simulation of the incoming shortwave radiation under cloudless conditions, and the estimation of the effects of clouds with three different parametrisation of the irradiance reduction. Main ancillary components used in the paper are the JGrass-V and the Kriging components, used, respectively for the verification of the results, and the spatial interpolation of irradiance reduction characteristics.

The outputs provided by the model composition shown are independent of both the simulation time step and of the spatial resolution the user want to use. This mean that they can be integrated in both semi-distributed hydrological model and for fully distributed hydrological model (once these models follow the conditions required by OMS3).

The theoretical formulation of the model composition used in the paper is tested by using three datasets from different watersheds (different geomorphological and climatological features) with good results as quantified by some objective indexes.

The model, as made by OMS3 components is able to use all of the Jgrass-NewAge components such as the GIS visualization tools inherited from uDig (http://udig.refractions.net), and being connected to other components, for calibration of the parameters, estimation of long wave radiation, evapotranspiration and discharge, and for snow modelling, as presented in Formetta et al. (2011).

Further the paper shows some possibility offered by the modelling by components paradigm in envisioning various possible analyses obtained by the composition of different modelling components in the pool of the ones of the JGrass-NewAGE system.

If another parameterisation of the same radiation processes will be introduced in the future, it will simply constitute an alternative component that that could be inserted by adding or eliminating it from the simulation script just before the run-time, without altering any other piece of the modelling solution.

GMDD
5, 4355–4393, 2012

Acknowledgement. This paper has been partially produced with financial support from the HydroAlp project, financed by the Province of Bolzano. The Authors thanks Andrea Antonello and Silvia Franceschi (Hydrologis) and Daniele Andreis for their work on preliminary versions of parts of the codes.

References

Allen, P. and Naney, J.: Hydrology of the Little Washita River Watershed, Oklahoma: Data and Analyses. USDA-ARS, ARS-90. December, 1991. 4366

Bird, R. and Hulstrom, R.: Simplified clear sky model for direct and diffuse insolation on horizontal surfaces, Tech. rep., Solar Energy Research Inst., Golden, CO (USA), 1981. 4361

Boland, J., Scott, L., and Luther, M.: Modelling the diffuse fraction of global solar radiation on a horizontal surface, Environmetrics, 12, 103–116, 2001. 4365

Corripio, J.: Modelling the energy balance of high altitude glacierised basins in the Central Andes., Ph.D. dissertation, University of Edinburgh, 2002. 4359, 4360, 4362, 4363, 4368, 4379

Corripio, J.: Vectorial algebra algorithms for calculating terrain parameters from DEMs and solar radiation modelling in mountainous terrain, Int. J. Geogr. Inf. Sci., 17, 1–24, 2003. 4357, 4359, 4360

David, O., Markstrom, S., Rojas, K., Ahuja, L., and Schneider, I.: The object modeling system. Agricultural system models in field research and technology transfer, Press LLC, Chapter 15, 317- 333, 2002. 4358

David, O., Ascough, J., Leavesley, G., and Ahuja, L.: Rethinking modeling framework design: object modeling system 3.0, in: IEMSS 2010 International Congress on Environmental Modeling and Software Modeling for Environments Sake, Fifth Biennial Meeting, July 5–8, 2010, Ottawa, Canada; Swayne, Yang, Voinov, Rizzoli, and Filatova (Eds.), 1183–1191, 2010. 4358

Donatelli, M., Carlini, L., and Bellocchi, G.: A software component for estimating solar radiation, Environ. Model. Softw., 21, 411–416, 2006. 4358

Dozier, J. and Frew, J.: Rapid calculation of terrain parameters for radiation modeling from digital elevation data, IEEE T. Geosci. Remote, 28, 963–969, 1990. 4357

Dubayah, R.: Modeling a solar radiation topoclimatology for the Rio Grande River Basin, J. Veg. Sci., 5, 627–640, 1994. 4357

GMDD

5, 4355–4393, 2012

Dubayah, R. and Paul, M.: Topographic solar radiation models for GIS, Int. J. Geogr. Inf. Sys., 9, 405–419, 1995. 4358
Duguay, C.: Radiation modeling in mountainous terrain review and status, Mountain Research and Development, 13, 339–357, 1993. 4357
Erbs, D., Klein, S., and Duffie, J.: Estimation of the diffuse radiation fraction for hourly, daily and monthly-average global radiation, Solar Energy, 28, 293–302, 1982. 4364
Formetta, G., Mantilla, R., Franceschi, S., Antonello, A., and Rigon, R.: The JGrass-NewAge system for forecasting and managing the hydrological budgets at the basin scale: models of flow generation and propagation/routing, Geosci. Model Dev., 4, 943–955, doi:10.5194/gmd-4-943-2011, 2011. 4358, 4365, 4369, 4373, 4374
Formetta, G., Chavez, J., David, O., and Rigon, R.: Shortwave radiation variability on complex terrain., in preparation, Geosci. Model Dev., 2013. 4358, 4373
Fu, P. and Rich, P.: The solar analyst 1.0 user manual, Helios Environmental Modeling Institute, 1616 Vermont St KS, 66044 USA, 2000. 4358
Goovaerts, P.: Geostatistics for Natural Resources Evaluation, Oxford University Press, USA, 1997. 4365
Gubler, S., Gruber, S., and Purves, R. S.: Uncertainties of parameterized surface downward clear-sky shortwave and all-sky longwave radiation., Atmos. Chem. Phys., 12, 5077–5098, doi:10.5194/acp-12-5077-2012, 2012. 4358
Gupta, H., Kling, H., Yilmaz, K., and Martinez, G.: Decomposition of the mean squared error and NSE performance criteria: implications for improving hydrological modelling, J. Hydrol., 377, 80–91, 2009. 4370
Helbig, N., Löwe, H., Mayer, B., and Lehning, M.: Explicit validation of a surface shortwave radiation balance model over snow-covered complex terrain, J. Geophys. Res.-Atmos., 115, D18113, 2010. 4363
Hetrick, W., Rich, P., Barnes, F., and Weiss, S.: GIS-based solar radiation flux models, in: ACSM ASPRS Annual Convention, 3, 132–132, American Soc. Photogr. Remote Sens. + Amer. Cong. on Bethesda, Maryland, 1993. 4358
Hofierka, J. and Suri, M.: The solar radiation model for Open source GIS: implementation and applications, Proceedings of the Open source GIS – GRASS users conference 2002 – Trento, Italy, 11–13 September 2002. 4358
Hoyt, D.: A model for the calculation of solar global insolation, Solar Energy, 21, 27–35, 1978. 4363

GMDD
5, 4355–4393, 2012

Iqbal, M.: An Introduction to Solar Radiation, 1983. Academic Press, Orlando, FL, USA. 4357, 4361, 4362, 4363, 4368
Jones, J., Keating, B., and Porter, C.: Approaches to modular model development, Agric. Sys., 70, 421–443, 2001. 4358
Liou, K.: An Introduction to Atmospheric Radiation, 84, Academic Press USA, 2002. 4357
Long, C. N. and Ackerman, T. P.: Surface Measurements of Solar Irradiance: A Study of the Spatial Correlation between Simultaneous Measurements at Separated Sites, J. Appl. Meteorol., 34, 1039–1046, doi:10.1175/1520-0450(1995)034<1039:SMOSIA>2.0.CO;2, 1995. 4368, 4373
Miklánek, P.: The estimation of energy income in grid points over the basin using simple digital elevation model, in: Ann. Geophys., 11, European Geophysical Society, Springer, 1993. 4358
Miller, R.: The jackknife – a review, Biometrika, 61, 1–15, 1974. 4372
Moore, I.: SRAD: direct, diffuse, reflected short wave radiation, and the effects of topographic shading. Terrain Analysis Programs for Environmental Sciences (TAPES) Radiation Program Documentation, Center for Resource and Environmental Studies, Australia National University, Canberra, Australia, 1992. 4358
Orgill, J. and Hollands, K.: Correlation equation for hourly diffuse radiation on a horizontal surface, Solar Energy, 19, 357–359, 1977. 4364
Prata, A.: A new long-wave formula for estimating downward clear-sky radiation at the surface, Q. J. Roy. Meteorol. Soc., 122, 1127–1151, 1996. 4362
Quenouille, M.: Notes on bias in estimation, Biometrika, 43, 353–360, 1956. 4372
Ranzi, R. and Rosso, R.: Distributed estimation of incoming direct solar radiation over a drainage basin, J. Hydrol., 166, 461–478, 1995. 4357
Reindl, D., Beckman, W., and Duffie, J.: Diffuse fraction correlations, Solar Energy, 45, 1–7, 1990. 4364, 4365, 4371
Rizzoli, A., Svensson, M., Rowe, E., Donatelli, M., Muetzelfeldt, R., Wal, T., Evert, F., and Villa, F.: Modelling framework (SeamFrame) requirements, Report No. 6, SEAMLESS integrated project, EU 6th Framework Programme, contract no. 010036-2, www.SEAMLESS-IP.org, 49 pp., ISBN 90-8585-034-7. 2005. 4358
Rogers, J.: Environmental and water resources: milestones in engineering history: 15–19 May 2007, Amer. Society of Civil Engineers, Tampa, Florida, 2007. 4366
Spencer, J.: Fourier series representation of the position of the sun, Search, 2, 172- 218, 1971. 4360

GMDD
5, 4355–4393, 2012

Stehr, A., Debels, P., Romero, F., and Alcayaga, H.: Hydrological modelling with SWAT under conditions of limited data availability: evaluation of results from a Chilean case study, Hydrol. Sci. J., 53, 588–601, 2008. 4372

Tovar, J., Olmo, F., and Alados-Arboledas, L.: Local-scale variability of solar radiation in a mountainous region, J. Appl. Meteorol., 34, 2316–2328, 1995. 4367, 4368, 4373

Van Liew, M., Arnold, J., and Bosch, D.: Problems and potential of autocalibrating a hydrologic model, Trans. ASAE, 48, 1025–1040, 2005. 4372

Wilson, J. and Gallant, J.: Terrain Analysis: Principles and Applications, Wiley, New York, 2000. 4358

GMDD

5, 4355–4393, 2012

Table 1. List of the SwRB component parameter used in simulations.

Symbol	Parameter description	Dimension	Values
l_{oz}	vertical ozone layer thickness	[cm]	0.30
V	visibility, Corripio (2002)	[km]	80.0
ω_0	single-scattering albedo fraction of incident energy scattered to total attenuation by aerosols	[–]	0.9
F_s	fraction of forward scattering to total scattering	[–]	0.84

GMDD
5, 4355–4393, 2012

Table 2. List of the meteorological stations used in the simulations performed on Little Washita river basin. ID is the station identificative number, City is the closer city to the station, LAT and LONG stand for latitude and longitude, respectively, Elevation and Aspect are the station elevation and aspect, respectively. Bold font is used for indicating the stations belonging to the validation set.

ID	City	LAT.	LONG.	Elevation (m)	Aspect (°)
124	**Norge**	**34.9728**	**–98.0581**	**387.0**	**138°**
131	Cyril	34.9503	–98.2336	458.0	245°
133	Cement	34.9492	–98.1281	430.0	116°
134	Cement	34.9367	–98.0753	384.0	65°
135	Cement	34.9272	–98.0197	366.0	182°
136	Ninnekah	34.9278	–97.9656	343.0	270°
144	Agawam	34.8789	–97.9172	388.0	50°
146	Agawam	34.8853	–98.0231	358.0	212°
148	**Cement**	**34.8992**	**–98.1281**	**431.0**	**160°**
149	Cyril	34.8983	–98.1808	420.0	205°
150	**Cyril**	**34.9061**	**–98.2511**	**431.0**	**195°**
153	Cyril	34.8553	–98.2121	414.0	165°
154	Cyril	34.8553	–98.1369	393.0	175°
156	Agawam	34.8431	–97.9583	397.0	290°
159	Rush Springs	34.7967	–97.9933	439.0	235°
162	Sterling	34.8075	–98.1414	405.0	15°
182	**Cement**	**34.845**	**–98.0731**	**370.0**	**245°**

GMDD
5, 4355–4393, 2012

Table 3. List of the meteorological stations used in the simulations performed on Fort Cobb river basin. ID is the station identificative number, City is the closer city to the station, LAT and LONG stand for latitude and longitude, respectively, Elevation and Aspect are the station elevation and aspect, respectively. Bold font is used for indicating the stations belonging to the validation set.

ID	City	LAT.	LONG.	Elevation (m)	Aspect (°)
101	**Hydro**	**35.4551**	**–98.6064**	**504.0**	**120°**
104	Colony	35.3923	–98.6233	484.0	35°
105	**Colony**	**35.4072**	**–98.571**	**493.0**	**300°**
106	Eakly	35.3915	–98.5138	472.0	295°
108	Eakly	35.3611	–98.5712	492.0	40°
109	**Eakly**	**35.3123**	**–98.5675**	**466.0**	**90°**
110	Eakly	35.3303	–98.5202	430.0	115°
113	Colony	35.291	–98.6357	465.0	155°

GMDD
5, 4355–4393, 2012

Table 4. List of the meteorological stations used in the simulations performed on Arabba river basin. ID is the station identificative number, City is the closer city to the station, LAT and LONG stand for latitude and longitude, respectively, Elevation and Aspect are the station elevation and aspect, respectively. Bold font is used for indicating the stations belonging to the validation set.

ID	City	LAT.	LONG.	Elevation (m)	Aspect (°)
1	Arabba	46.4999	11.8761	1825	180°
2	**Caprile**	**46.4404**	**11.9900**	**1025**	**170°**
3	Agordo	46.2780	12.0331	602	5°
8	Villanova	46.4433	12.2062	972	71°
9	**Auronzo**	**46.5562**	**12.4258**	**940**	**223°**
11	Campo di Zoldo	46.3466	12.1841	915	160°
12	Domegge di Cadore	46.4609	12.4103	802	148°
14	Monte Avena	46.0321	11.8271	761	55°
18	Passo Pordoi	46.4834	11.8224	357	55°
21	Passo Monte Croce	46.6521	12.4239	1612	120°
22	Col Indes	46.1191	12.4401	1119	210°
23	**Torch**	**46.1515**	**12.3629**	**602**	**177°**
26	Sappada	46.5706	12.7080	1275	156°
29	Feltre	46.0162	11.8946	273	190°
31	Falcade	46.3554	11.8694	1151	50°
32	Cortina	46.536	12.1273	1244	88°
35	Belluno	46.1643	12.2450	378	157°

GMDD
5, 4355–4393, 2012

Table 5. Index of goodness of fit between modelled and measured solar radiation on Little Washita river basin.

STATION ID	KGE	MAE [W m^{-2}]	PBIAS [%]
148	0.94	16.65	4.90
124	0.95	17.50	3.80
182	0.98	16.50	1.80
150	0.97	17.90	2.10

GMDD
5, 4355–4393, 2012

Table 6. Index of goodness of fit between modelled and measured solar radiation on Fort Cobb river basin.

STATION ID	KGE	MAE [W m^{-2}]	PBIAS [%]
101	0.96	15.6	5.5
105	0.95	13.50	2.80
109	0.97	14.07	2.70

GMDD
5, 4355–4393, 2012

Table 7. Index of goodness of fit between modelled and measured solar radiation on Arabba river basin.

STATION ID	KGE	MAE	PBIAS
2	0.92	4.53	2.7
9	0.89	22.10	14.80
23	0.95	3.58	2.1

GMDD
5, 4355–4393, 2012

Table 8. List of symbols.

Symbol	Name	Unit
c_d	Adjustement coefficient for $d\downarrow$	[–]
c_s	Adjustment coefficient for $S\downarrow$	[–]
$d\downarrow$	Total diffuse irradiance	[W m^{-2}]
$d\downarrow_r$	Diffuse irradiance component due to Raileigh's scattering	[W m^{-2}]
$d\downarrow_a$	Diffuse irradiance component due to aerosol scattering	[W m^{-2}]
$d\downarrow_m$	Diffuse irradiance component due to multiple reflections	[W m^{-2}]
k_d	Ratio between the global irradiance and the ???	[–]
k_t	Clearness sky index	[–]
l_o	Vertical ozone layer thickness	[cm]
m_a	Relative air mass	[–]
m_r	Relative optical air mass	[–]
w	Precipitation water	[cm]
p	Air pressure	[mb]
$C_1 = 0.9751$	Constant in equation (1)	[–]
E_0	Correction for Earth's orbit eccentricity	[–]
F_c	Forward scattering to total scattering	[–]
I_{sc}	Solar constant	[W m^{-2}]
$\hat{I}_{sc}$	Modified solar constant	[W m^{-2}]
N	Day number	[–]
$R\downarrow_{sw}$	Total incident direct radiation on a sloping surface	[W m^{-2}]
$R\downarrow^*_{sw}$	Correct irradiance for direct shortwave radiation on a sloping surface	[W m^{-2}]
$\hat{R}\downarrow^*_{sw}$	Measured total irradiance from direct shortwave radiation at meteo-stations	[W m^{-2}]
$S\downarrow$	Incident direct shortwave radiation on a sloping surface	[W m^{-2}]
$S\downarrow^*$	Incident direct shortwave radiation on a sloping surface	[W m^{-2}]
T_s	Products of atmospheric transmittances	[–]
V	Visibility	[km]
V_s	Sky-view factor	[–]
α_a	Albedo of the cloudless sky	[–]
α_g	Ground albedo	[–]
β_s	Correction factor for increasing of transmittance with elevation	[–]
κ	Day angle	[rad]
θ_s	Angle between Sun vector and surface tangent plane	[rad]
θ_z	Zenit angle	[rad]
ψ	Shadows index	[–]
τ_r	Raileigh's scattering transmittance	[–]
τ_0	Ozone transmittance	[–]
τ_g	Uniformly mixed gases transmittance	[–]
τ_w	Water vapour transmittance	[–]
τ_a	Aerosols transmittance	[–]
τ_{aa}	Transmittance of direct radiation due to aerosol absorptance	[–]
τ_{as}	$:= \tau_a \tau_{aa}^{-1}$	[–]
ω_0	Single scattering albedo fraction	

GMDD
5, 4355–4393, 2012

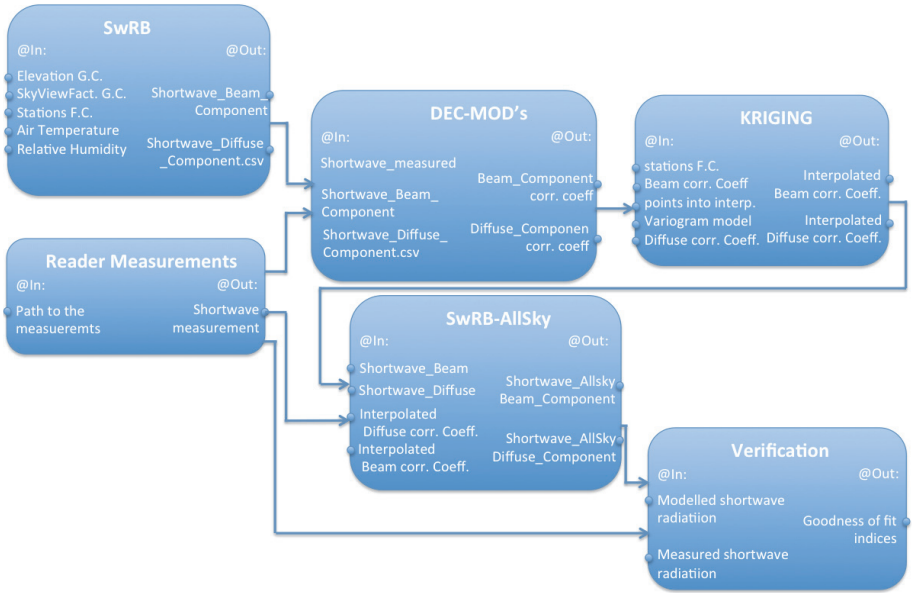

Fig. 1. OMS3 SWRB components of JGrass-NewAge and flowchart to model shortwave radiation at the terrain surface with generic sky conditions. Where not specified, quantity in input or output must be intended as a spatial field for any instant of simulation time. "Measured" refers to a quantity that is measured at a meteorological station. Geomorphic features refer to the hilllslope and channel delineation, slope and aspect. The components, besides the specfied files received in input, include an appropriate set of parameter values.

GMDD
5, 4355–4393, 2012

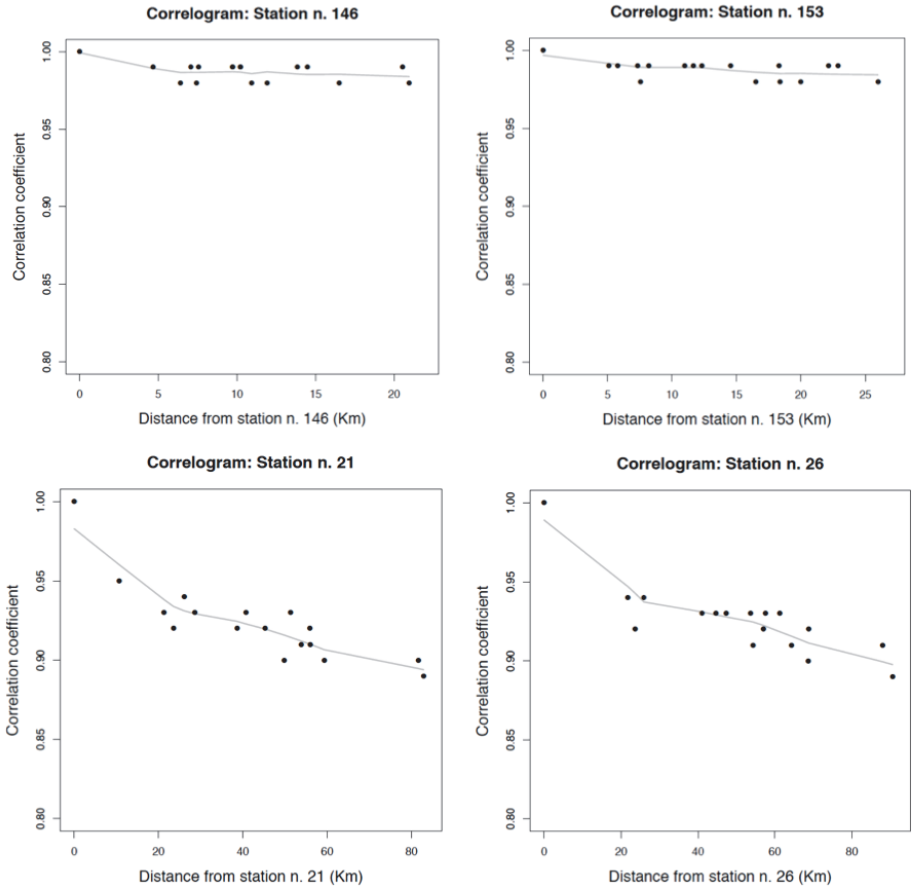

Fig. 2. Correlogram between station 146 and 159 and station on Little Washita river basin, at the top. Correlogram for station 21 and 26 on Piave river basin, at the bottom.

GMDD
5, 4355–4393, 2012

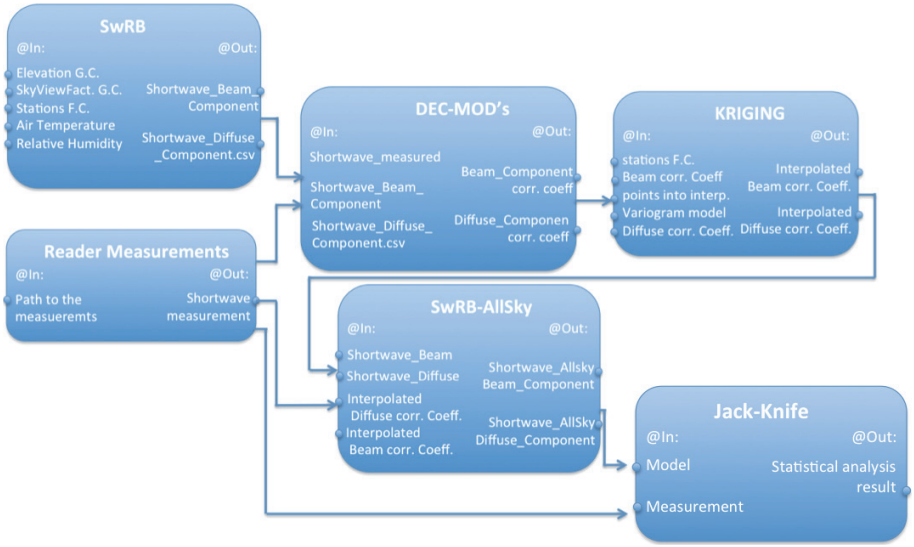

Fig. 3. OMS3 SWRB components of JGrass-NewAge and flowchart for automatic Jack-Knife procedure.

GMDD
5, 4355–4393, 2012

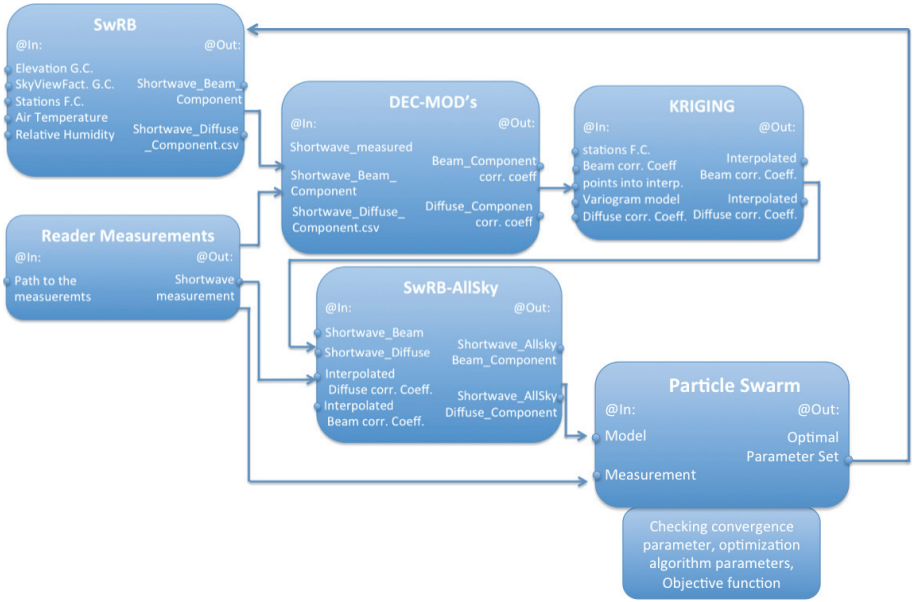

Fig. 4. OMS3 SWRB components of JGrass-NewAge and flowchart for model parameter calibration.

GMDD
5, 4355–4393, 2012

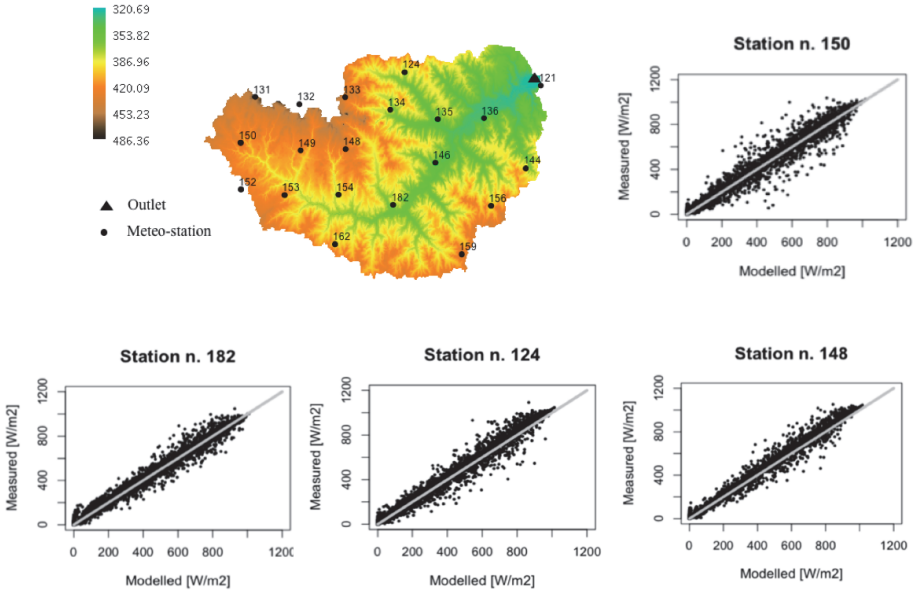

Fig. 5. The Little Washita river basin, Oklahoma (USA).

GMDD
5, 4355–4393, 2012

Modeling short wave solar radiation using the JGrass-NewAge system

G. Formetta et al.

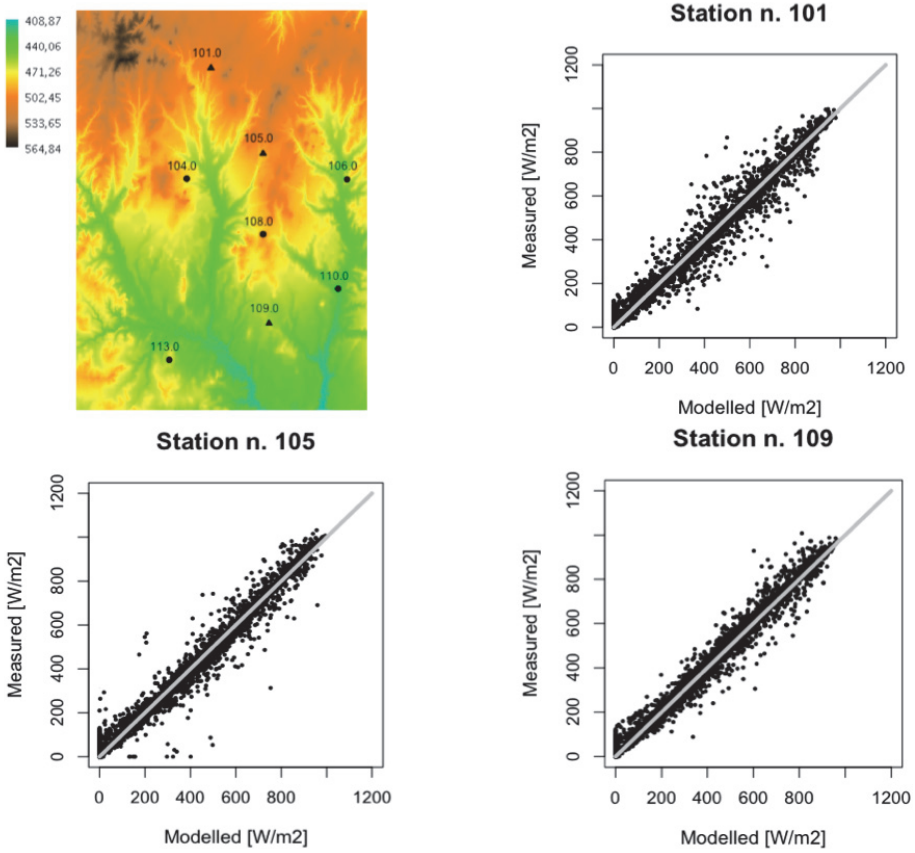

Fig. 6. The Fort Cobb river basin results.

GMDD
5, 4355–4393, 2012

Modeling short wave solar radiation using the JGrass-NewAge system

G. Formetta et al.

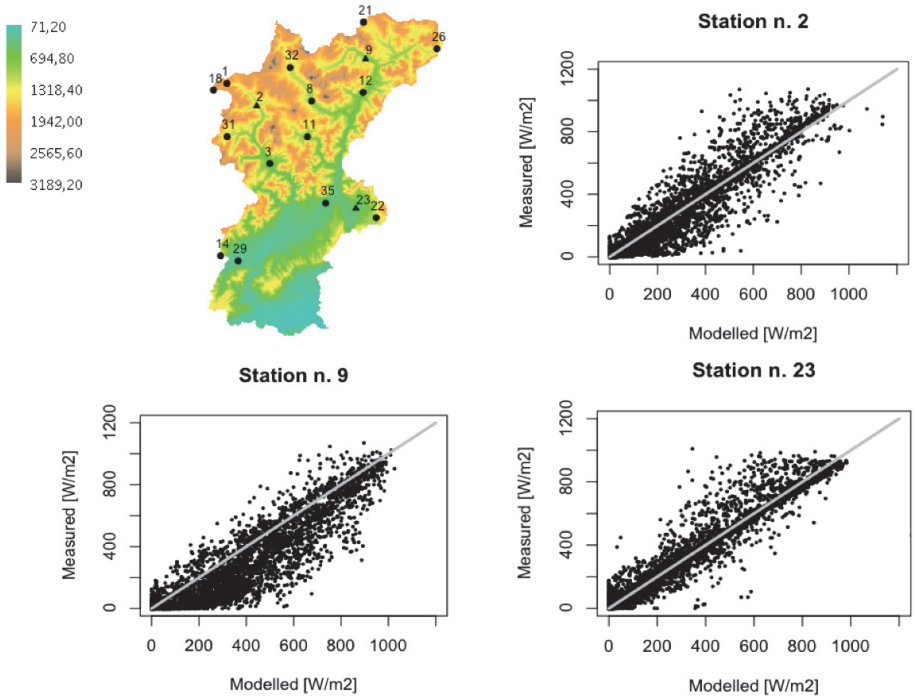

Fig. 7. River Piave area (Italy).

GMDD
5, 4355–4393, 2012

Modeling short wave solar radiation using the JGrass-NewAge system

G. Formetta et al.